

Surface topography effects on galling of hot dip galvanized sheet metal

VENEMA Jenny^{1,a*}, CHEZAN Toni^{1,b} and KORVER Frank^{1,c}

¹Tata Steel, Research & Development, PO BOX 10000, 1970 CA IJmuiden, The Netherlands

^ajenny.venema@tatasteelurope.com, ^btoni.chezan@tatasteelurope.com,

^cfrank.korver@tatasteelurope.com

Keywords: Tribology, Friction, Wear, Zinc Coatings, Galling, Automotive

Abstract. During manufacturing of automotive parts from hot dip galvanized sheet metal, surface asperities of the forming tools can cause breakage of small coating particles. Long and narrow scratches appear on the surface of the form part, a phenomenon known as part surface galling. Laboratory testing using a slider on sheet tests (SOST) are performed in order to investigate surface topography effects on galling. These experiments reveal the dominant effect of tool surface roughness on galling. The tool surface roughness has a large effect on the size of the detached coating particles and the distance before scratch occurrence. If the tool roughness is low enough, no surface scratch formation is observed for the investigated range of sheet surface roughness. At a high tool surface roughness scratches are observed at a very short sliding distance for all tested materials. At an intermediate tool surface roughness, the materials selected for this investigation show measurable differences but no clear trend could be identified.

Introduction

Galling, abrasive surface wear of hot dip galvanized steel (GI) sheet metal can occur during deep drawing, the process commonly used for automotive part manufacturing. Observations of industrial forming processes in the areas with contact with the forming tools revealed two types of contact conditions – normal contact and galling. In normal contact conditions the sheet metal topography is flattened by the tool contact. Such contact areas on the deformed sheet surface can be considerably large, tens of millimeters in the sliding length direction, as the sheet metal slides against the forming tools. In some contact areas unexpected galling behavior in the form of long narrow scratches, in the sheet metal sliding direction [1] was observed. Such scratches are created by tool surface local asperities. The consequence of surface scratch formation might be coating detachment in the form of thin flakes. The flakes might attach to the tool surface resulting in increased tool asperity height and in formation of new tool surface asperities and consequently in acceleration of galling of the following formed part.

In the industry several solution directions exist to prevent galling, namely polishing, hardening and/or coating the forming tool surface and/or the application of extra lubrication. These solution directions indicate already some of the parameters which influence galling, such as tool surface parameters such as roughness and lubrication. Other parameters which influence galling are sheet surface, design (deformation) and process parameters such as pressure, velocity and temperature. In the literature investigations on the mechanisms of galling and the influence of several parameters can be found [2-5]. For example, Van de Heide and Dane [6-7] investigated the influence of lubricant on galling.

In a previous investigation [1] the influence of pressure and tool roughness on galling was investigated with the Slider On Sheet Tester (SOST) on one material with representative roughness. In the current investigations the influence of the tool roughness is investigated for three sheet material roughness levels within the typical intervals found in automotive applications. Both the scratch depth and particle sizes are investigated in great detail.

Material and Methods

An experimental program was started to evaluate the geometrical surface parameter on galling. The experiments were performed using a SOST capable of providing controlled well-defined contact conditions between the tool surface and metal sheet. Tests were performed on three different GI coated steel sheets and three different tool roughness levels (Table 1). The tribological interactions were studied by Scanning Electron Microscopy (SEM) analysis of particles collected from the tool. The dimensional topography measurements of the tool and sheet surfaces were performed by a confocal microscope.

Table 1. Surface parameters of the sheet and tool material according to ISO 25178.

	Sa [μm]	Sq [μm]	Sz [μm]	Ssk [-]	Sku [-]	Sp [μm]	Sv [μm]
Tool ring 1	0.33	0.43	5.22	-0.43	4.25	2.66	2.55
Tool ring 2	0.74	0.99	11.96	-1.27	8.45	3.39	8.55
Tool ring 3	1.19	1.57	15.30	-0.97	4.89	6.89	8.42
Sheet 1	1.00	1.14	6.64	0.45	2.50	3.85	2.79
Sheet 2	1.17	1.36	7.73	-0.08	2.06	3.92	3.81
Sheet 3	1.59	1.89	12.30	-0.42	2.30	6.62	5.70

A cylindrical tool (Fig.1a) with contact width of 6 mm is pressed with 1.5 bar (resulting in a normal load of 205 N) against the sheet material. The contact situation is therefore a line contact, with a nominal pressure of 190 MPa. The cylinder moves in length direction for 250 mm at a velocity of 50 mm/s, lifted up and brought into a new position to make a new track next to the previous one (Fig.1b) within a few seconds. In this way, every time virgin sheet material is in contact with the tool. The amount of tracks is depended on the tool roughness and availability of material (sheet size). For the smoothest tool (Sa 0.3 μm), between 70 and 75 tracks are tested, resulting in 17.5 to 18.8 m sliding length for the three different materials. This sliding length can represent drawing of approximately close to 200 parts. The tool is rotated (approximately 5°) after each unique parameter setting. In this way a fresh tool material is in contact for each test. A pressure sensitive foil is used to align the tool properly, thereby ensuring homogeneous contact at the start of the test.

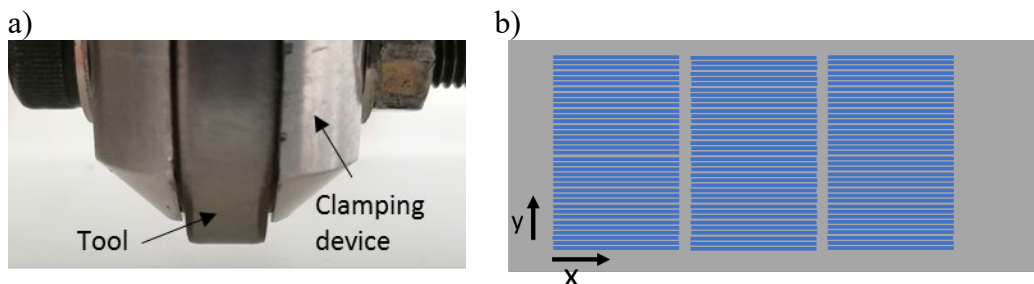


Fig. 1. a) Photograph of cylindrical tool (half) in SOST b) Schematic view of sheet with tracks.

Three different GI coated steel sheets (thickness 0.6 mm) with different surface roughness are tested (Fig. 2). The sheets are cleaned with isopropanol to remove mill applied lubricant on the surface.

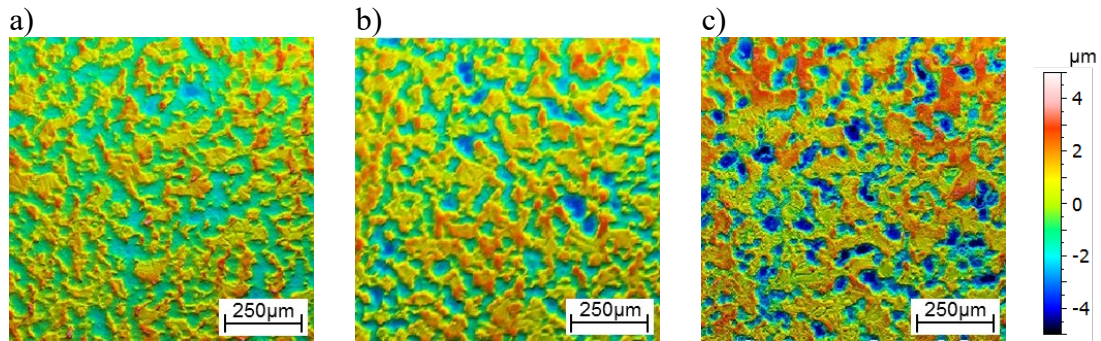


Fig. 2. Confocal measurement sheet surface (size 1x1 mm) a) Sa 1.0 μm b) Sa 1.2 μm c) Sa 1.6 μm .

The slider (diameter of 43 mm) of tool material DIN 1.2379 has a hardness of 60 ± 2 HRC. Three different tool textures with different roughness (Fig. 3) are tested. The tool surface topography has a defined lay with the grinding direction perpendicular to sliding direction.

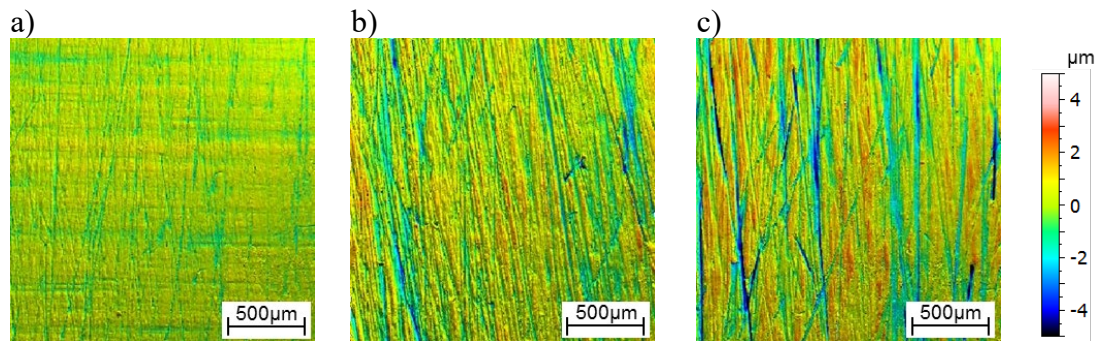


Fig. 3. Confocal measurement tool surface (2x2 mm) a) Sa 0.3 μm b) Sa 0.7 μm c) Sa 1.2 μm . Sliding direction is horizontal.

Results and Discussion

The appearance of the scratches, ploughing tracks and particles are similar to observations on automotive pressed parts and particles collected from stamping tools [1]. The tool wear mechanism is dynamic. Particles of the GI coating break out during sliding and get trapped in different types of tool surface defects (such as grinding scratches). They stick to the tool surface (Fig.4a & 4b). During repeated sliding the particle build up accumulates. Particle accumulation can cause scratches to sheet material, which can become more severe with sliding distance. However, it is also observed that particles break off resulting in a disappearing scratch or a less severe scratch. The process will continue and the particle accumulation will start again at the same or at another position. Loose particles can also cause 3rd body abrasive wear. These scratches do not necessarily follow the same direction as the sliding direction, but could bend off. This wear mechanism was also observed in a few cases in earlier investigations.

In general, the thickness of individual flakes is lower than the thickness of the GI coating and the GI coating is not spalling off. In case of highest tool roughness the scratch depth becomes close to the thickness of the zinc coating. Cross sectional microscopy is planned to further investigate the fracture of the zinc coating.

After the test the particles were collected with adhesive tape for further investigation in the SEM (Fig. 4c). Mapping of the elements of the particles reveals that it mainly consists of Zn (Fig. 4d) and some coating elements (Al). In general, no tool material elements such as Cr are measured. This indicates that no abrasive tool wear occurs. Also, in most cases almost no Fe is measured, suggesting that the scratches are superficial.

The tools are ultrasonic cleaned after collection of the particles. After ultrasonic cleaning of the tools, some Zn particles are still attached to the tool surface (Fig. 4b) in which the sliding direction is visible. Remaining particles on the slider after ultrasonic cleaning represents well the industrial case in which grinding is necessary to remove all particles.

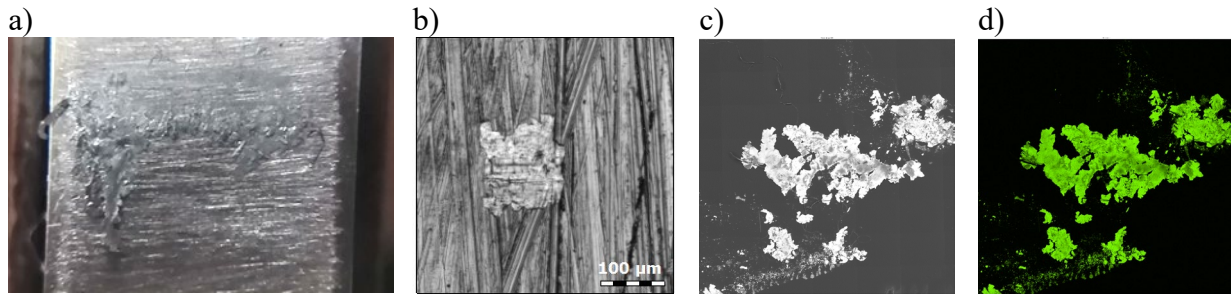


Fig. 4. a) Photo of contact surface of tool after test (tool width 6 mm) b) particle remained after ultrasonic cleaning of tool c) SEM BSE collected particles from tool (size 8.5 x 8.5 mm) Tool Sa 0.7 μm Sheet Sa 1.2 μm. SEM /EDX element mapping of Zn (L) (size 8.5 x 8.5 mm) Tool Sa 0.7 μm Sheet Sa 1.2 μm.

Particles collected from tool.

The collected particles are in the majority of the cases flakes, for one material also some other particle morphology is observed. These flakes are very comparable to the flakes collected from industrial tools at OEMs (Fig. 5). The flakes are only a few microns thick, while the width and length are more than 10 times the thickness.

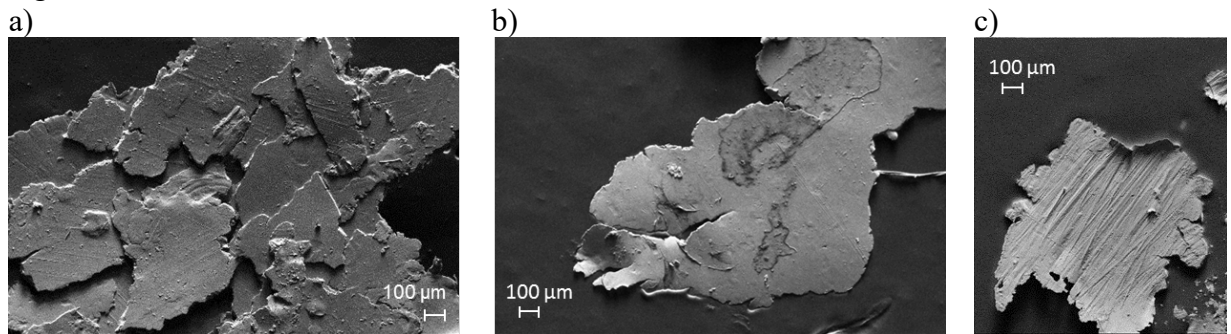


Fig. 5. SEM images a) particles collected from industrial tool b) one particle collected from industrial tool c) one particle collected from SOST sheet Sa 1.2 μm tool Sa 1.2 μm.

The size of the flakes is dependent on the surface roughness, and the average size increases in the majority of cases with increasing tool roughness (Fig. 6).

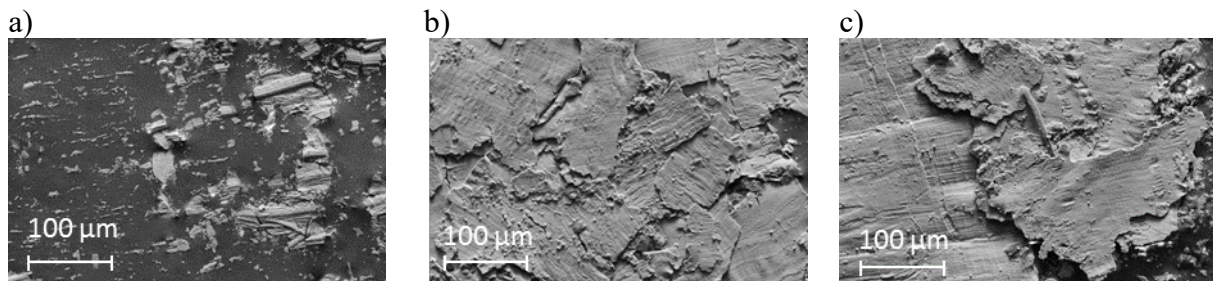


Fig. 6. SEM analysis of particles after test sheet Sa 1.6 μm with tool roughness a) Sa 0.3 μm b) Sa 0.7 μm c) Sa 1.2 μm.

Scratches on the sheet surface.

Three dimensional topography measurements are made at specific track numbers (1,10,20,40,60 and last track). A 2D profile cross section is created and the maximum profile depth determined (Fig. 7a). Criterion for a scratch is a larger than 1 μm increase in max profile depth compared to original material. Fig. 7b shows the maximum profile depth versus the sliding distance for sheet material 1 ($S_a=1.0 \mu\text{m}$) for several tool roughness. In case of low tool roughness ($0.3 \mu\text{m}$) no scratch occurs. At medium tool roughness ($0.7 \mu\text{m}$) scratch occurs at 15 m of sliding distance. And for a high tool roughness ($1.2 \mu\text{m}$) the scratch occurs immediately after start of test. Thus, the tool roughness plays a major effect on the distance to scratch formation.

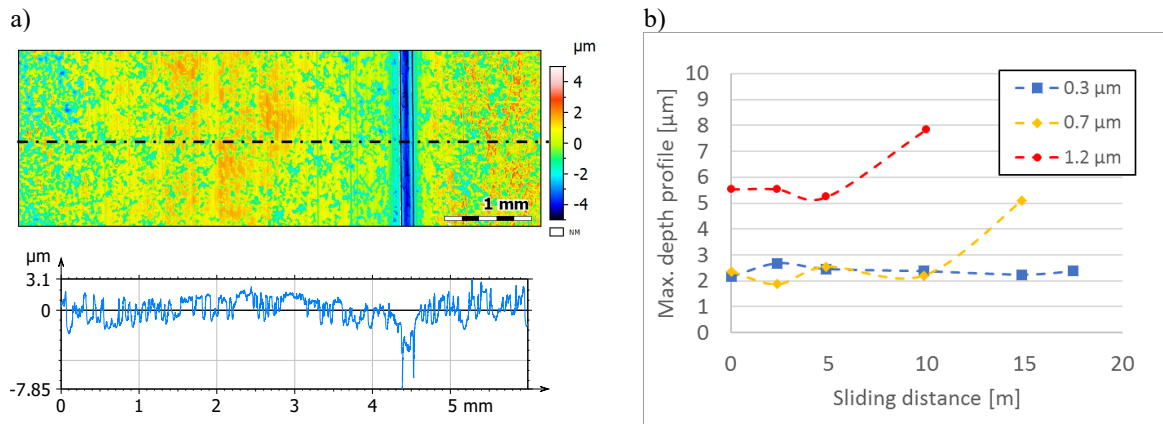


Fig. 7. A) 3D topography measurement sheet $S_a 1.0 \mu\text{m}$ tool $S_a 1.2 \mu\text{m}$ after 10 m sliding. b) max. profile depth versus sliding distance sheet $S_a 1.0 \mu\text{m}$ for the tested tool textures.

For the entire collection of sheet materials no scratches are observed for a low tool roughness of $0.3 \mu\text{m}$ (Table 2). This shows that the sheet coating can resist relative high contact conditions in case of smooth surface.

In case of intermediate tool roughness the distance before a scratch occurs was different for the three materials considered in this study. A more extended experimental research is necessary to further quantify the sheet coating effect. Also, the number of tests is very limited and further investigations are necessary to determine the range in distance before scratch occurrence for different sheet material and tool roughness combinations. However, trends regarding the increase in tool roughness are observed for each material and each test series (Table 2). An increase in tool roughness results in a decrease in distance to scratch (Table 2) which is probably related to the larger particle size and the presence of more tool surface defects to get stuck. Larger particles can probably be less easily removed out of the contact.

Table 2. Distance [m] to first measured scratch.

Tool roughness S_a	Sheet roughness S_a		
	1.0 [μm]	1.2 [μm]	1.6 [μm]
0.3 [μm]	>17.5	>18.8	>18.5
0.7 [μm]	14.9	4.9	9.9
1.2 [μm]	0.0	2.4	2.4

Fig. 8 reveals the dynamic nature of galling. For example, at a tool roughness of $0.7 \mu\text{m}$ a large scratch occurs at track 20, which becomes less severe at track 60. Indicating that a part of the adhered particles broke off from the tool. In case of a roughness of $1.2 \mu\text{m}$ the position of the scratches also changes, indicating that the buildup and breaking of particles on the tool can occur at several position on the tool.

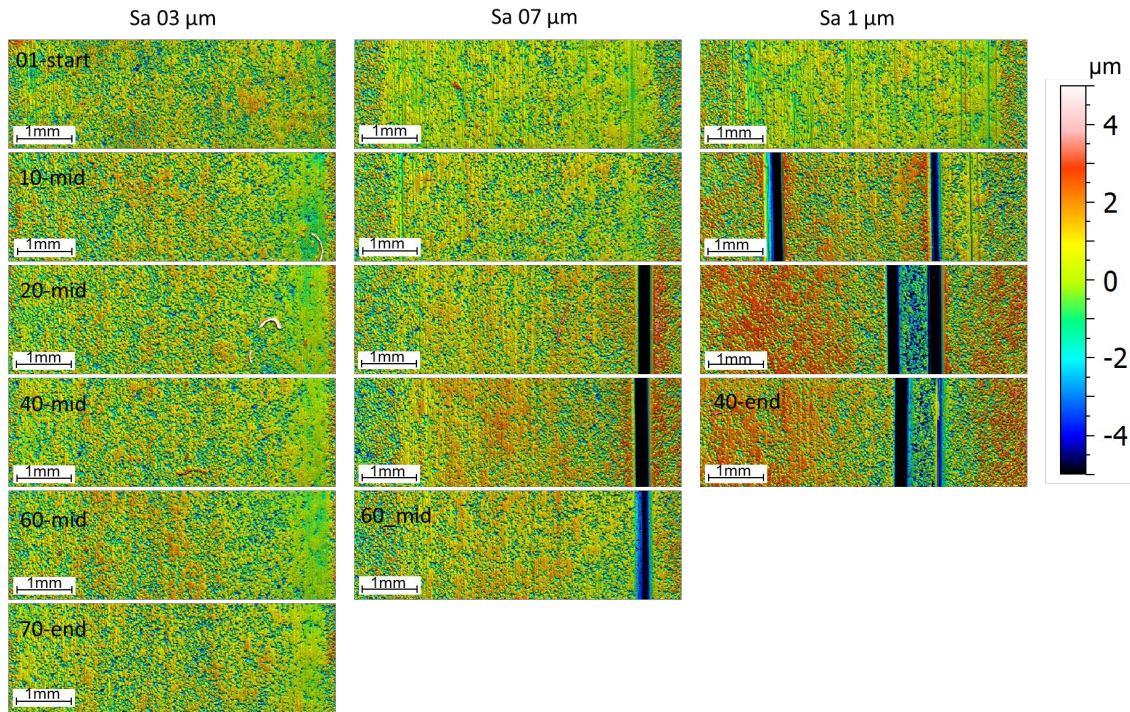
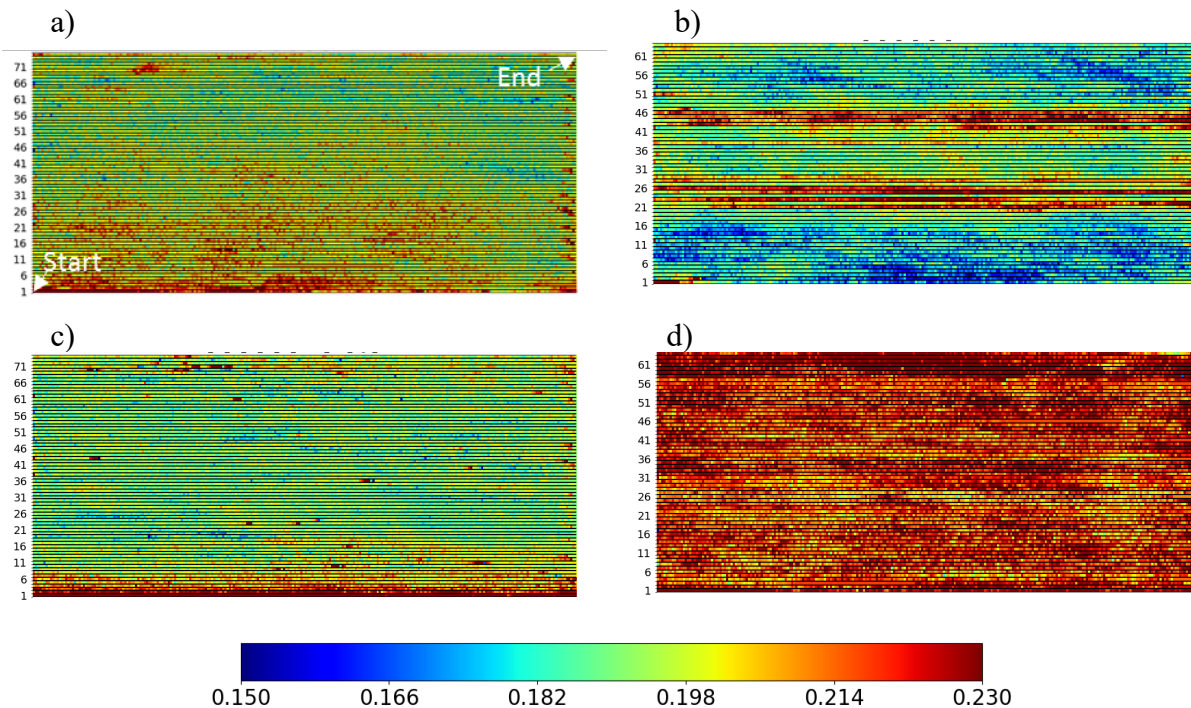


Fig. 8. Confocal measurements for sheet material 2 ($Sa 1.2 \mu\text{m}$) at positions (# tracks) and for three tool roughness . Sliding in vertical direction.

Coefficient of Friction (COF).

The effect of tool roughness on the COF is also high (Fig.9). With a low tool roughness the friction coefficient is stable and relatively low. Sometimes a certain increase and decrease in COF is related to a scratch, however this certainly is not always the case. The friction coefficient is higher or lower with increasing tool roughness. A different wear regime (cut, wear or ploughing) could cause a different trend in friction coefficient. Recommended is to investigate this effect further with a physical based friction model.



*Fig. 9. Colour plot coefficient of friction for the tracks a) Tool Sa 0.3 μm Sheet Sa 1.2 μm
b) Tool Sa 0.7 μm Sheet Sa 1.2 μm c) Tool Sa 0.3 μm Sheet Sa 1.6 μm
d) Tool Sa 0.7 μm Sheet Sa 1.6 μm .*

Summary

The experiments reveal the dominant effect of tool surface roughness on galling of the sheet metal coating. It was found that the detached coating flake size increases with increasing tool surface roughness. A too low or too high tool surface roughness resulted in either no surface scratch formation or deep surface scratches after very short sliding distance for all tested sheet materials. The roughness magnitude of the sheet metal surface appeared to influence the galling resistance performance as well for the tests with intermediate tool surface roughness. The material roughness magnitude differences were less clear while compared to the tool surface roughness effect. Further investigations are planned focused on material coating parameters effect on galling performance.

Acknowledgements

The authors would like to thank Ronald van Goethem, Arne Neelen and Marco Appelman for surface measurement and Jan Wörmann for the SEM analysis.

References

- [1] J. Venema, F. Korver, T. Chezan, Slider on Sheet Tester Development for Characterizing Galling, ESAFORM 2022, Key Eng. Mater. 926 (2022) 1204–1210. <https://doi.org/10.4028/p-iii69m>
- [2] E. Schedin, Galling mechanisms in sheet forming operations, Wear 179 (1994) 123-128. [https://doi.org/10.1016/0043-1648\(94\)90229-1](https://doi.org/10.1016/0043-1648(94)90229-1)
- [3] H. Kim, J. Sung, F.E. Gondwin, T. Altan, Investigation of galling in forming galvanized advanced high strength steels (AHSSs) using the twist compression test (TCT), J. Mater. Process. Technol. 205 (2008) 459-468. <https://doi.org/10.1016/j.jmatprotec.2007.11.281>
- [4] W. Wang, K. Wang, Y. Zhao, M. Hua, X. Wei, A study on galling initiation in friction coupling stretch bending with advanced high strength hot-dip galvanized sheet, Wear 328-329 (2015) 286–294. <http://doi.org/10.1016/j.wear.2015.02.058>

- [5] K.G. Budinski, S.T. Budinski, Interpretation of galling tests, *Wear* 332-333 (2015) 1185-1192.
<https://doi.org/10.1016/j.wear.2015.01.022>
- [6] E. van der Heide, A.J. Veld, D.J. Schipper, The effect of lubricant selection on galling in a model wear test, *Wear* 251 (2001) 973-979.
- [7] C.M. Dane, E. van der Heide, Proceedings of the IDDRG '04 Conference, Sindelfingen, Germany, 2004, pp. 182-191.